

## ENCIT-2018-0815

# DETERMINATION OF THE DISTRIBUTION OF TEMPERATURES IN PERMANENT REGIME OF AN ELECTRONIC SYSTEM THROUGH FINITE DIFFERENCE

### **Daniel Zancanella de Camargo**

Instituto Federal do Espírito Santo, Department of Mechanical Engineering,  
Rod. BR 101 Norte, km 58, Litorâneo, São Mateus, Espírito Santo, Brazil.  
danielzancanella@hotmail.com

### **Matheus Alves Lima**

Instituto Federal do Espírito Santo, Department of Mechanical Engineering,  
Rod. BR 101 Norte, km 58, Litorâneo, São Mateus, Espírito Santo, Brazil.  
matheus13.limma@gmail.com

### **Lorena Lúcia Bastos Bandeira**

Instituto Federal do Espírito Santo, Department of Mechanical Engineering,  
Rod. BR 101 Norte, km 58, Litorâneo, São Mateus, Espírito Santo, Brazil.  
bastoslorenna@gmail.com

### **Lucky Vieira Barcelos**

Instituto Federal do Espírito Santo, Department of Mechanical Engineering,  
Rod. BR 101 Norte, km 58, Litorâneo, São Mateus, Espírito Santo, Brazil.  
lucky.barcelos@gmail.com

### **Luan Lenke de Paula**

Instituto Federal do Espírito Santo, Department of Mechanical Engineering,  
Rod. BR 101 Norte, km 58, Litorâneo, São Mateus, Espírito Santo, Brazil.  
luanlenke@gmail.com

**Abstract.** *The use of a silicon electronic chip especially when driving and controlling a DC motor, causes an increase in the equipment's temperature and influences its performance and data processing. Determining the temperature distribution throughout the system ensures the proper use and extends the chip's life within its temperature limiting conditions. This study proposes a numerical solution of one heat transfer model of the chip using the finite difference method (FDM) applied for permanent regime for the original chip and simulating its substrate increasing in size, aiming optimization. Based on the results obtained, it is observed that the system has a temperature distribution within the manufacturer's specifications and that increasing the dielectric substrate's size contributes to the reduction of the heat transfer by convection.*

**Keywords:** *silicon chip, dielectric substrate, temperature, heat transfer.*

## 1. INTRODUCTION

Understanding the mechanisms of heat transfer is increasingly important, playing a decisive role in generating several elements of daily. Its field of application goes from biological systems to common home appliances, for residential and commercial buildings, industrial processes and food processing. Heat exchangers, condensers, radiators, heaters, ovens, refrigerators and solar energy collectors are some of the equipment designed based on the heat transfer analysis (Çengel, 2009).

With the information technology revolution in recent decades, important discoveries have been made possible through advances in thermal engineering, allowing accurate temperature control in nanotechnology systems. These advances, at present, are limited because of the difficulty of cooling tiny devices (Incropera *et al.*, 2008).

The field of research related to the heat transfer in electronic systems is ample due to its range of applications. Reis (2013) analyzes thermal heat sinks for electronic components in aeronautical equipment. Schuh (2017) assesses thermal efficiency for a high-performance processor from various physical construction configurations.

In most thermal analysis problems, in practice there will always be elements with complex geometry and contour conditions that are difficult to simplify or consider. In this case, the use of numerical methods is required. According to

Çengel (2009), numerical methods present approximate solutions that are accurate enough through the use of computers. There are several ways to obtain a numerical formulation, they can be by the method of finite differences, finite elements, contour elements and control volume. Schuh (2017) and Reis (2013) use the finite number method in control volumes, applying computational simulations through ANSYS.

Such numerical methods are not used only for the electronics field. Silva (2004) performed a biotransfer of heat analysis in ocular tissues using the finite volume method while Júnior *et al.* (2014) apply the finite difference method in a biotransfer of heat model in living tissue based on porous environment. Santos (2008) developed a thermal model for solution in heat transfer in turning processes.

The use of electronic systems (chip), mainly to drive and control a DC motor, causes the heating of the equipment and influences its performance and data processing. The purpose of this study is to obtain the temperature distribution in permanent regime for a chip as well as the heat dissipation for the external environment analyzed for two different value of the dielectric substrate's height. The chip was used in a motor drive shield coupled with an Arduino® board for controlling the position of a DC motor's shaft.

## 2. MATERIALS AND METHODS

The chip-substrate system presents some fundamental characteristics: the surfaces are in contact with the external ambient while the other sides are isolated from the ambient. The electrical power dissipation on the chip provides uniform volumetric heating at a rate of heat transfer ( $\dot{q}$ ). The geometry also shows symmetry in the center and, for simplification of the equations, this property is used.

In order to carry out the study, the following considerations were made:

- The system is very long in the perpendicular direction, adopting a two-dimensional model;
- Constant properties;

The temperature field is analyzed in the cross-sectional area of the system as shown in Fig. 1.

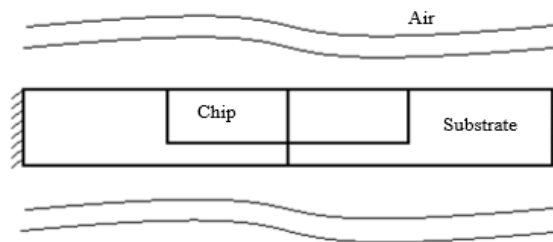


Figure 1. Transversal area of the system.

Chip and substrate data were acquired from datasheets of equipment and other information platforms provided by manufacturers. The substrate considered is FR4 Glass-reinforced epoxy type and the Dual Full Bridge driver type L298P (Power SO20) according to Tab. 1 and Tab. 2.

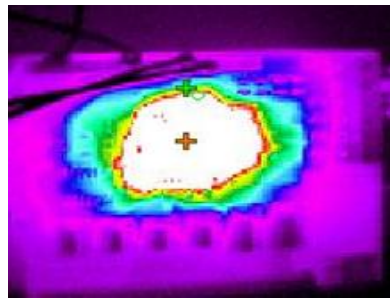
Table 1. Properties of the substrate.

Data	Symbol	Value	Unity
Thermal conductivity	$K_S$	0,343	W/mK
Height	H1	1,8	mm
Length	L	53,34	mm
Maximum operating temperature	$T_{SMAX}$	140	°C

Table 2. Properties of the chip.

Data	Symbol	Value	Unity
Thermal conductivity	$K_C$	149	W/mK
Height	h	3,6	mm
Length	l	16,2	mm
Thickness	e	1,6	mm
Maximum operating temperature	$T_{CMAX}$	150	°C
Internal generation	$\dot{q}$	39,457E6	W/m <sup>3</sup>

Through a thermographic inspection report, Fig. 2, the temperatures around and at the center of the system was determined so that the contour conditions for computational modeling could be defined.



Temperature measurement

Cursor 1	59.9 °C
Cursor 2	100.2 °C
Difference	-40.3 °C

Figure 2. Thermographic inspection report.

Due to the symmetry of the system, only the right half of the system was analyzed. In order to determine the size of the mesh, a size corresponding to the dimensions of the geometry of the system was chosen, thus adopting a mesh with a spacing of 1.8 mm (both horizontally and vertically). Consequently, we could represent the part of the analyzed system with a total of 44 nodes according to Fig. 3.

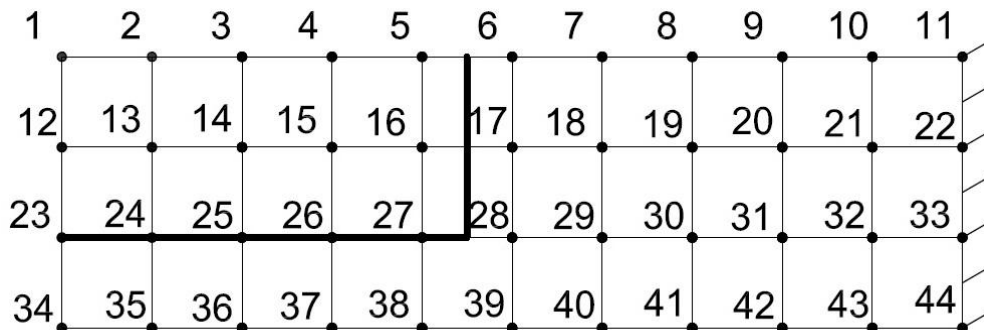
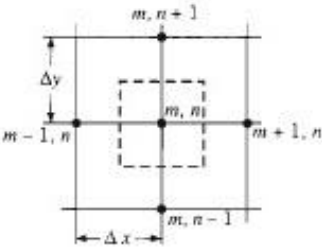
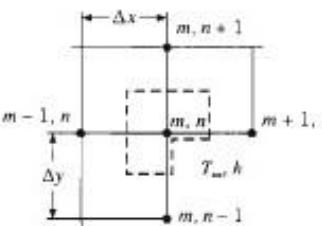
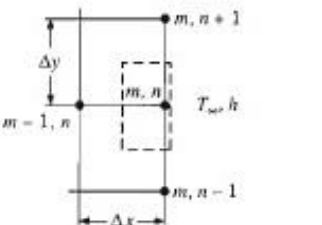
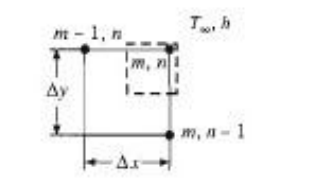
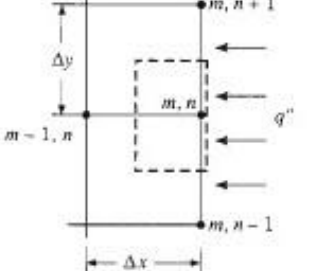


Figure 3. Distribution of the nodes in the mesh.

In order to obtain a temperature distribution, the finite difference equation can be obtained by applying the energy balance method at each node. By increasing the height of the substrate by a further spacing of 1.8 mm below, the part of the system to be analyzed increases to a total of 55 nodes.

In order to solve the finite difference equations, the Engineering Equation Solver (EES) software was used for the chip with the original dielectric substrate, and the iterative Gauss-Seidel method was used for the optimized substrate.

Configuration	Finite-Difference Equation for $\Delta x = \Delta y$
	$T_{m,n+1} + T_{m,n-1} + T_{m+1,n} + T_{m-1,n} - 4T_{m,n} = 0$ <p><b>Case 1. Interior node</b></p>
	$2(T_{m-1,n} + T_{m,n+1}) + (T_{m+1,n} + T_{m,n-1}) + 2\frac{h\Delta x}{k}T_{\infty} - 2\left(3 + \frac{h\Delta x}{k}\right)T_{m,n} = 0$ <p><b>Case 2. Node at an internal corner with convection</b></p>
	$(2T_{m-1,n} + T_{m,n+1} + T_{m,n-1}) + \frac{2h\Delta x}{k}T_{\infty} - 2\left(\frac{h\Delta x}{k} + 2\right)T_{m,n} = 0$ <p><b>Case 3. Node at a plane surface with convection</b></p>
	$(T_{m,n-1} + T_{m-1,n}) + 2\frac{h\Delta x}{k}T_{\infty} - 2\left(\frac{h\Delta x}{k} + 1\right)T_{m,n} = 0$ <p><b>Case 4. Node at an external corner with convection</b></p>
	$(2T_{m-1,n} + T_{m,n+1} + T_{m,n-1}) + \frac{2q''\Delta x}{k} - 4T_{m,n} = 0$ <p><b>Case 5. Node at a plane surface with uniform heat flux</b></p>

<sup>a,b</sup>To obtain the finite-difference equation for an adiabatic surface (or surface of symmetry), simply set  $h$  or  $q''$  equal to zero.

Figure 4. Distribution of the nodes in the mesh.  
 Source: Incropera *et al.*, 2008.

### 3. RESULTS

The equations used to find the nodal point temperatures were based on Incropera *et al.* (2008) (Fig. 4) and by energy balances (Eq. 1 to 7) to another cases that was not specified.

$$T_{m-1,n} + T_{m+1,n} + 2T_{m,n-1} - 2\left(\frac{h_{ar}\Delta x}{k_c} + 2\right)T_{m,n} + 2\frac{h_{ar}\Delta x}{k_c}T_{\infty} + \frac{q'''\Delta x\Delta y}{k_c} = 0 \quad (1)$$

$$T_{m-1,n} + 2\left(1 + \frac{k_s}{k_c}\right)T_{m+1,n} + 2T_{m,n-1} - \left(5 + \frac{k_s}{k_c} + 2\frac{h_{ar}\Delta x}{k_c}\right)T_{m,n} + 2\frac{h_{ar}\Delta x}{k_c}T_{\infty} + \frac{q'''\Delta x\Delta y}{k_c} = 0 \quad (2)$$

$$2\left(1 + \frac{k_c}{k_s}\right)T_{m-1,n} + T_{m+1,n} + 2T_{m,n-1} - \left(5 + 2\frac{k_c}{k_s} + 2\frac{h_{ar}\Delta x}{k_s}\right)T_{m,n} + 2\frac{h_{ar}\Delta x}{k_c}T_{\infty} = 0 \quad (3)$$

$$T_{m,n+1} + T_{m-1,n} + T_{m+1,n} + T_{m,n-1} - 4T_{m,n} + \frac{q'''\Delta x\Delta y}{k_c} = 0 \quad (4)$$

$$T_{m,n+1} + T_{m-1,n} + 2\left(1 + \frac{k_s}{k_c}\right)T_{m+1,n} + T_{m,n-1} - \left(5 + 2\frac{k_s}{k_c}\right)T_{m,n} + \frac{q'''\Delta x\Delta y}{k_c} = 0 \quad (5)$$

$$T_{m,n+1} + T_{m+1,n} + 2\left(1 + \frac{k_c}{k_s}\right)T_{m-1,n} + T_{m,n-1} - \left(5 + 2\frac{k_c}{k_s}\right)T_{m,n} = 0 \quad (6)$$

$$2T_{m,n+1} + 2\left(\frac{k_s}{k_c}\right)T_{m,n-1} + \left(1 + \frac{k_s}{k_c}\right)T_{m-1,n} + \left(1 + \frac{k_s}{k_c}\right)T_{m+1,n} - 4\left(1 + \frac{k_s}{k_c}\right)T_{m,n} + \frac{q'''\Delta x\Delta y}{k_c} = 0 \quad (7)$$

In nodes, which the heat transfer is given by convection from the external fluid, conduction of the neighboring nodes and internal heat generation due to the chip is used to Eq. 1. Those that are observed convection, conduction between the materials and internal heat generation, are governed by Eq. 2, in a similar case but without generation, was used the Eq. 3 (for nodes 5 and 6, respectively). The Equation 4 is used for nodes only with conduction and power generation, in the case of the same configuration but between materials, we used Eq. 5. Now for nodes with the conduction of the substrate and the chip simultaneously was used Eq. 6 and for the nodes that are exactly at the chip-substrate border the temperature can be found by Eq. 7.

The Fig. 5 shows the heat maps generated with the solutions of the developed equations, the top map (a) represents the original system and the bottom map (b) with the substrate system increased.

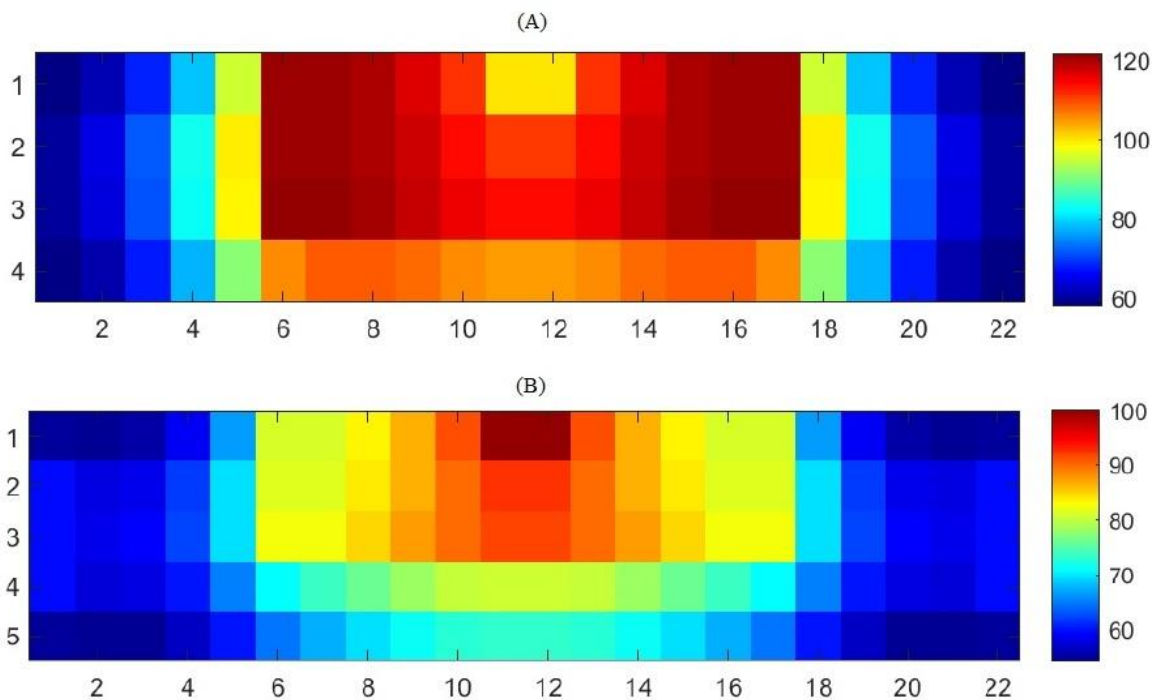


Figure 5. Heat map generated (temperatures in Celsius).

Can be observed, in the second case that the heat transfer by convection decrease. This occurred because the heat transfer by conduction was intensified by the substrate increase and Eq. 8 gives the convection dissipation

$$\dot{q} = h \sum_i A(T_i - T_{\infty}) \quad (8)$$

It is shown that for the original substrate the heat dissipation by convection was about 58 W and for the system with height increased by 1.8 mm a value of 34.97 W was obtained.

#### **4. CONCLUSION**

For the permanent regime without substrate increase, the system presented temperature distribution within the manufacturers' operating specifications. The increase of the substrate contributed significantly to the dissipation of the heat generated inside the chip and proved to be an adequate alternative for the improvement of the operation and processing of the chip and other electrical circuits since it has decreased the temperature in the nodes.

#### **5. ACKNOWLEDGEMENTS**

Acknowledgments to Instituto Federal do Espírito Santo for support during research.

#### **6. REFERENCES**

- Çengel, Y. A. *Transferência de calor e massa: uma abordagem prática*. 3. ed. São Paulo: McGraw - Hill, 2009.
- Incropera, F. P., Dewitt, D. P., Bergman, T. L. and Lavine, A. S., 2008. *Fundamentos de transferência de calor e massa*. 6<sup>th</sup> ed. Rio de Janeiro: LTC. 643 p.
- Júnior, K. G. F., Loureiro, F. dos S. and Reis, R. F., 2014. *Uma Aplicação do Método das Diferenças Finitas com Funções de Base Radial em Problemas de Biotransferência de Calor*. XI Simpósio de Mecânica Computacional e II Encontro Mineiro de Modelagem Computacional, Juiz de Fora.
- Reis, F. G. dos, 2013. *Análise de dissipadores térmicos para componentes eletrônicos de alta potência em um equipamento embarcado em aeronave*. Monografia. Universidade Federal do Rio Grande do Sul. Porto Alegre.
- Santos, M. R. dos, 2008. *Modelo térmico para a solução de problemas inversos em transferência de calor com aplicação em um processo de usinagem por torneamento*. Dissertação (mestrado). Universidade Federal de Uberlândia. Uberlândia.
- Schuh, M. O., 2017. *Caracterização e análise térmica de um microprocessador de alta performance via método numérico*. Monografia. Universidade Federal do Rio Grande do Sul. Porto Alegre.
- Silva, G. M. L. L. da, 2004. *Análise da biotransferência de calor nos tecidos oculares devido à presença de implantes retinianos através da utilização do método dos volumes finitos em malhas não estruturadas*. Dissertação (mestrado). Universidade Federal de Pernambuco, Recife.

#### **7. RESPONSIBILITY NOTICE**

The authors are the only responsible for the printed material included in this paper.